

Integrative analysis of mitochondrial and immune pathways in diabetic kidney disease: identification of AASS and CASP3 as key predictors and therapeutic targets

Xinxin Yu^{a,b,‡}, Yongzheng Hu^{a,‡} and Wei Jiang^a

^aDepartment of Nephrology, The Affiliated Hospital of Qingdao University, Qingdao, Shandong, China; ^bDepartment of Nephrology, Qingdao Eighth People's Hospital, Qingdao, Shandong, China

ABSTRACT

Objectives: Diabetic kidney disease (DKD) is driven by mitochondrial dysfunction and immune dysregulation, yet the mechanistic interplay remains poorly defined. This study aimed to identify key molecular networks linking mitochondrial and immune pathways to DKD progression, with a focus on uncovering biomarkers and therapeutic targets.

Methods: We conducted an integrative analysis of human DKD cohorts (GSE30122, GSE96804) using weighted gene co-expression network analysis (WGCNA) to identify gene modules enriched for immune response genes and mitochondrial pathways (from MitoCarta3.0). Machine learning algorithms were employed to prioritize key biomarkers for further investigation. Experimental validation was performed using a DKD rat model.

Results: WGCNA revealed significant gene modules associated with immune responses and mitochondrial functions. Machine learning analysis highlighted two central biomarkers: aminoadipate-semialdehyde synthase (AASS) and caspase-3 (CASP3). In the DKD rat model, elevated levels of AASS and CASP3 were found to correlate with increased oxidative stress. Mechanistically, AASS was shown to drive mitochondrial damage via lysine metabolism, while CASP3 amplified inflammatory apoptosis pathways.

Conclusions: Our findings establish AASS and CASP3 as dual biomarkers and therapeutic targets, bridging mitochondrial-immune crosstalk to DKD pathogenesis. This multi-omics framework provides actionable insights for targeting kidney damage in diabetes.

ARTICLE HISTORY

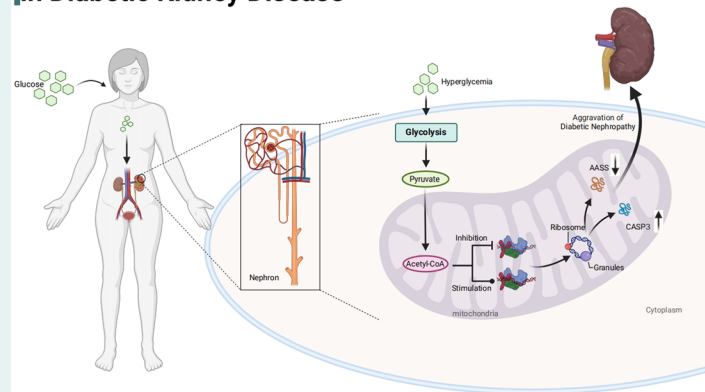
Received 3 July 2024
Revised 4 February 2025
Accepted 5 February 2025

KEYWORDS

Diabetic kidney disease (DKD); mitochondrial dysfunction; immune dysregulation; CASP3; AASS


GRAPHICAL ABSTRACT

Mitochondrial Dynamics in Diabetic Kidney Disease



CONTACT Wei Jiang  jiangwei866@qdu.edu.cn  Department of Nephrology, The Affiliated Hospital of Qingdao University, Qingdao, Shandong, China.

[‡]These authors contributed equally to this work and should be considered co-first authors.

 Supplemental data for this article can be accessed online at <https://doi.org/10.1080/0886022X.2025.2465811>.

This article has been corrected with minor changes. These changes do not impact the academic content of the article.

© 2025 The Author(s). Published by Informa UK Limited, trading as Taylor & Francis Group.

This is an Open Access article distributed under the terms of the Creative Commons Attribution-NonCommercial License (<http://creativecommons.org/licenses/by-nc/4.0/>), which permits unrestricted non-commercial use, distribution, and reproduction in any medium, provided the original work is properly cited. The terms on which this article has been published allow the posting of the Accepted Manuscript in a repository by the author(s) or with their consent.

Introduction

The global prevalence of diabetes mellitus (DM) is rising at an alarming rate [1], with diabetic kidney disease (DKD) emerging as one of the most significant complications contributing to chronic kidney disease and renal failure. DKD not only poses a substantial public health burden but also contributes extensively to morbidity and mortality worldwide [2,3]. Despite extensive research into the mechanisms of DM and its complications, the precise molecular pathways driving DKD remain incompletely understood.

Emerging evidence has highlighted mitochondrial dysfunction as a central factor in the pathogenesis of DKD, with disruptions in mitochondrial dynamics—such as fission, fusion, and mitophagy—playing critical roles in kidney cell injury, particularly in podocytes and proximal tubular cells [4]. These cells, crucial to renal function, are highly susceptible to mitochondrial perturbations, leading to energy deficits, cellular damage, and functional decline [5]. Studies have shown that mitochondrial dynamics—including processes such as fission, fusion, and mitophagy—are pivotal in maintaining podocyte health. Disruption of these processes can lead to podocyte injury [6]. Additionally, alterations in mtDNA, detectable in blood and urine, provide potential biomarkers for early-stage DKD [7]. However, while the role of mitochondrial dysfunction is increasingly recognized, the intricate interplay between mitochondrial abnormalities, immune responses, and DKD progression remains poorly understood.

Recent studies have emphasized the critical role of immune responses in conjunction with mitochondrial dysfunction in the progression of diabetic kidney disease (DKD). Immune cells, including macrophages and T cells, are central to the inflammatory processes that drive kidney injury in DKD. In the diabetic state, characterized by elevated cytokines, chemokines, and other pro-inflammatory mediators, these immune cells are activated, exacerbating renal damage [8]. Concurrently, mitochondrial dysfunction, a key driver of DKD, is aggravated by hyperglycemia. This includes alterations in mitochondrial DNA (mtDNA), disruption of the electron transport chain, and increased production of reactive oxygen species (ROS), all of which directly contribute to kidney cell injury [9]. However, the relationship is bidirectional: mitochondrial dysfunction not only damages kidney cells but also affects immune cell function, thereby establishing a vicious feedback loop. Furthermore, the persistent hyperglycemic environment in diabetic patients promotes the formation of advanced glycation end products (AGEs), which activate crucial signaling pathways such as MAPK and NF- κ B through their interaction with receptors like RAGE. These pathways further amplify oxidative stress and inflammation, exacerbating endothelial dysfunction and inflammatory processes within the kidney [10]. Moreover, immune cells are increasingly recognized for their role in sensing and responding to mitochondrial components released during cellular stress, which act as damage-associated molecular patterns (DAMPs). This recognition triggers additional inflammatory signaling, reinforcing the destructive cycle of mitochondrial dysfunction and immune activation in DKD [11]. Therapeutic strategies aimed at either targeting mitochondrial

dysfunction or modulating immune-mediated inflammation should be actively investigated.

Given these knowledge gaps, the current study aims to investigate the role of mitochondrial-related genes in the progression of DKD, with a particular focus on their relationship with immune cell infiltration. Bioinformatics has become an indispensable tool in advancing our understanding of DKD [12]. We employed an integrative bioinformatics approach, utilizing publicly available microarray data and advanced techniques such as weighted gene co-expression network analysis (WGCNA) and machine learning algorithms. WGCNA was used to identify gene modules that correlate with clinical traits of DKD, providing insights into the molecular landscape of the disease [13]. Machine learning further refined these results by predicting key regulatory genes, offering potential biomarkers or therapeutic targets for clinical intervention [14]. By analyzing datasets from the Gene Expression Omnibus (GEO), we were able to establish critical links between mitochondrial gene expression and immune cell populations, shedding light on the complex interactions between mitochondrial dysfunction and immune responses in DKD. This study aims to fill the critical gap in our understanding of the molecular mechanisms underlying DKD, with the ultimate goal of identifying novel therapeutic strategies to improve clinical outcomes.

Materials and methods

Microarray data retrieval

Microarray data for the investigation of DKD were sourced from the NCBI GEO repository (<http://www.ncbi.nlm.nih.gov/geo>) using the search terms 'diabetic nephropathy', 'Homo sapiens', and 'high throughput gene expression profile', which are relevant to kidney-related gene expression and diabetic conditions. The specific datasets used for bioinformatics analyses and machine learning model training were GSE30122 and GSE96804. The GSE30122 dataset ([HG-U133A_2] Affymetrix Human Genome U133A 2.0 Array) was generated *via* the GPL571 platform and contains 69 human kidney samples [15]. GSE30122 includes the GSE30528, GSE30529, and GSE30566 datasets. For the analysis of differentially expressed genes (DEGs) between diabetic nephropathy (DN) patients and control patients, 19 DN samples, including 9 glomerulus samples and 10 tubule samples, and 50 control human kidney samples were selected for analysis. The GSE96804 dataset ([HTA-2_0] Affymetrix Human Transcriptome Array 2.0) was generated *via* the GPL17586 platform and contains 61 human kidney samples from DN patients ($n=41$) and controls ($n=20$). GSE96804 served as the validation set, allowing for rigorous testing of the predictive algorithms developed in this study [16].

Annotation and differential gene expression analysis

Annotations for the probes utilized in the study were performed using the dataset's annotation files to ensure accurate gene identification. To establish the reliability of the dataset, principal component analysis (PCA) was performed to assess the reproducibility of the expression data using the base functionality in R software. Differential gene expression was

identified with the 'Limma' package (version 3.54.2) in R (version 4.2.3) statistical thresholds of a P value less than 0.05 and an absolute fold change (FC) greater than 1.0 were applied to select significant genes. Heatmaps and volcano plots were generated with the 'ComplexHeatmap' (version 2.15.4) and 'ggplot2' packages (version 3.4.3) in R to present the identified DEGs.

Weighted gene co-expression network analysis

Using the 'WGCNA' package (version 1.72-1) in R, we first subjected the differential expression data of 3,085 genes from 69 samples to standard bioinformatics preprocessing steps to ensure accurate and meaningful output [17]. A suitable soft threshold power, which is essential for constructing a scale-free network, was selected through the 'pickSoftThreshold' function, which optimizes network topology on the basis of scale independence and mean connectivity. Following the identification of an optimal soft threshold, we constructed a network using the 'blockwiseModules' function, specifying parameters including a minimum module size of 50 to ensure significant clustering and a merge cut height of 0.25 to combine closely related modules. This network not only mapped the intricate relationships among the genes contributing the top 25% of variance but also facilitated the identification of modules highly correlated with DKD traits. The module analysis was enriched with visualization tools in R such as 'plotDendroAndColors', which provided a dendrogram alongside the color-coded modules, vividly illustrating the clustering of genes and their module associations. Subsequent Pearson correlation analysis between module eigengenes and clinical traits of DKD offered insights into potential biomarkers or therapeutic targets.

Gene ontology (GO) and Kyoto encyclopedia of genes and genomes (KEGG) analyses

To explore the functional implications of the genes associated with DKD, enrichment analysis was conducted with the 'clusterProfiler' package in R, version 4.6.2. This analysis focused on the GO categories molecular function (MF), cellular component (CC), and biological process (BP) and KEGG pathways. This analysis was restricted to human genes. Enrichment outcomes were effectively visualized with bar plots to highlight significant interactions and functions. Only pathways and functions with an adjusted p value less than 0.05 were considered significantly enriched, confirming the biological relevance of the findings in the context of DKD.

Integration of mitochondrial genomics and network analysis

To deepen our understanding of mitochondrial dynamics in DKD, we utilized the MitoCarta3.0 database (<https://www.broadinstitute.org/mitocarta/mitocarta30-inventory-mammalian-mitochondrial-proteins-and-pathways>), which encompasses a meticulously curated inventory of 1,136 human genes [18]. This comprehensive database includes

proteins with robust evidence of mitochondrial localization derived from extensive mass spectrometry analyses of mitochondria isolated from fourteen different tissues. In our approach, these mitochondrial genes were integrated with the DKD-associated gene modules previously identified *via* WGCNA. Through Venn diagram analysis, we intersected the mitochondrial genes from MitoCarta3.0 with our WGCNA results to pinpoint crucial genes that may play pivotal roles in the mitochondrial pathophysiology of DKD.

Immune infiltration analysis

The 'Cibersort' package was used in R to quantify the immune cell composition from the gene expression data of DKD and control tissues [19]. This method allowed us to estimate the relative abundance of various immune cell types within the tissue samples. The results were graphically represented with bar graphs to depict the distribution of each immune cell type across the samples. Furthermore, violin plots facilitated the comparison of immune cell proportions between the DKD and control groups, providing visual insights into immune cell dynamics. Additionally, the relationships among the 22 types of infiltrating immune cells were illustrated through heatmaps generated with the 'corrplot' package in R, enhancing our understanding of the immune landscape in DKD.

Online clinical correlation analysis

To investigate the clinical significance of key genes in DKD, we utilized the Nephroseq V5 platform, which is accessible at Nephroseq (<http://v5.nephroseq.org/>). This resource is renowned for its integrative approach to data mining, linking genetic information with clinical phenotypes across various kidney diseases. Nephroseq V5 offers advanced analytical tools that enabled us to examine the correlations between the expression of selected hub genes and renal function metrics in DKD patients. We extracted expression data from two relevant datasets in the Nephroseq V5 repository, focusing specifically on patients diagnosed with DN. The data were then reanalyzed to produce scatter plots *via* the 'ggplot2' package (version 3.4.3) in R, facilitating a detailed visualization of gene expression correlations with clinical parameters.

Machine learning analysis

Using the 'randomForest' (RF) package (version 4.7-1.1) in R, we conducted a random forest (RF) analysis on the training dataset GSE30122 to identify genes with significant predictive power for DKD. This method evaluates the importance of variables by constructing multiple decision trees and aggregating their predictions. The importance scores for each gene were visualized *via* the varImpPlot function, highlighting the most relevant genes in DKD. The model's efficacy was validated on the test dataset GSE96804, and receiver operating characteristic (ROC) curves were plotted to assess the diagnostic performance, as indicated by the area under the ROC curve (AUC)

values, which revealed promising predictive capabilities. Following RF analysis, a support vector machine (SVM) was employed to enhance the feature selection process. This method, implemented with the `svm` function of the 'e1071' package (version 1.7-13), is particularly useful because of its ability to handle high-dimensional data. SVM models were trained and validated on the same datasets described above, with a focus on maximizing the margin between different classes of the response variable. ROC curves for the SVM model provided additional validation of the model's effectiveness. To complement the RF and SVM analyses, XGBoost was utilized because of its efficiency and performance in classification tasks. After the data were converted to DMATRIX format, an XGBoost model was trained using the 'xgb.train' function of the 'xgboost' package (version 1.7.5.1). This algorithm provides a robust framework for boosting tree algorithms and is highly effective in handling unbalanced data, which are prevalent in medical datasets. The importance of each feature was assessed via 'xgb.importance', and the results were visualized to identify the most influential genes.

Animal models and sampling

Ten male Wistar rats, each weighing between 250 and 300 grams, were obtained from Shandong Helix Biotechnology Co., Ltd., for use in this study. The rats were acclimated for one week in the animal laboratory of the Affiliated Hospital of Qingdao University. During this period, the room was maintained at 24°C with a 12-h light/dark cycle, and the rats were given unrestricted access to food. The Medical Ethics Committee of the Affiliated Hospital of Qingdao University approved all the experimental protocols (QYFY-WZLL-28888). The rats were randomly allocated into two groups: five rats were designated as the normal control group, and five rats constituted the DKD group. Following a 12-h fasting period, the DKD group received a single intraperitoneal injection of streptozotocin (STZ) (55 mg/kg body weight; Sigma-Aldrich, St. Louis, MO, USA) dissolved in sodium citrate buffer (pH 4.5). The control group was administered an equivalent volume of sodium citrate buffer. One week after injection, blood glucose levels were measured from tail vein samples collected on three consecutive days with an Accu-Chek glucometer (Roche Diagnostics, Indianapolis, IN, USA). The rats were considered diabetic if their plasma glucose levels were ≥ 16.67 mmol/L. Eight weeks after injection, the creation of an early DKD model was confirmed by assessing the urine protein-to-creatinine ratio. Urine was collected over a 24-h period in metabolic cages. At the end of the study, blood samples were obtained from all the rats from the orbital venous plexus following anesthesia with isoflurane. The complete data of the measured blood glucose levels and urine protein and creatinine levels are shown in Table S1. The rats were subsequently sacrificed under isoflurane anesthesia. Kidney tissues were promptly harvested, snap-frozen in liquid nitrogen, and stored at -80°C . To account for potential individual variability due to environmental and other factors, each sample was collected in triplicate.

ROS level determination in rat serum

Serum samples were thawed at 4°C and diluted to a suitable concentration (1:10) with PBS. To assess the ROS levels, 10 μM DCFDA from the ROS ELISA Kit (Shanghai FANKEW, Cat. No F9689-B) was added to each serum sample. The samples were incubated at 37°C for 30 min in the dark to allow DCFDA to be oxidized by ROS to form the fluorescent compound DCF. After incubation, the serum samples were briefly centrifuged at 3000 \times g for 5 min to remove any debris. One hundred microlitres of the supernatant from each sample was transferred to a 96-well plate, and fluorescence was measured at an excitation wavelength of 485 nm and an emission wavelength of 530 nm using a Multiskan Sky microplate reader (Thermo Fisher). The optical density (OD) values in the experimental group were normalized to those of the control group to assess the relative ROS levels.

RT-PCR validation of hub genes

According to our analysis results, we verified the expression levels of five key genes (MRPL49, caspase-3 [CASP3], EFHD1, amino adipate-semialdehyde synthase [AASS], and MPC1) in kidney samples from DN and control rats. Total RNA was extracted using TRIzol Reagent (Jiangsu CoWin Biotec, CW0580S, China) following the manufacturer's protocol, which involved tissue homogenization, phase separation with chloroform, and RNA precipitation with ethanol. The isolated RNA was reverse transcribed into cDNA using Evo M-MLV RT Premix (Accurate Biology, AG11706, China) at 37°C for 15 min and 85°C for 5 s. Quantitative real-time PCR (qRT-PCR) was conducted using a SYBR® Green Premix Pro Taq HS qPCR Kit (Accurate Biology, AG11701, China) on an ABI 7500 PCR system (ABI, Waltham, MA, USA). The reaction mixture included 2X SYBR Green Pro Taq HS Premix, specific primers for the target genes, and ROX Reference Dye. The thermal cycling conditions were as follows: initial denaturation at 95°C for 30 s, followed by 40 cycles of 95°C for 5 s and 60°C for 30 s and a dissociation stage to verify specificity. Relative expression levels were determined via the $2^{-\Delta\Delta\text{Ct}}$ method and normalized to the level of glyceraldehyde 3-phosphate dehydrogenase (GAPDH). The primer sequences for each gene were synthesized by Beijing Dingguo Biotechnology. The primer sequences are shown in Table 1.

Table 1. Primer sequences used for quantitative real-time PCR (qPCR).

| Gene | Real time-PCR primer sequences | |
|--------|--------------------------------|--------------------------|
| | Sequence | 5'-3' |
| AASS | Forward | TGGCTCACAACACTACAGGAACA |
| | Reverse | AGATGATGATGGCGACTTAACAC |
| CASP3 | Forward | GGAGCTTGGAAACGCGAAGAA |
| | Reverse | ACACAAGCCCATTTTCAGGGT |
| EFHD1 | Forward | AGGATCTGGAGAGGATGTTCAA |
| | Reverse | AGCAGCAGCCTTTGTGGAA |
| MPC1 | Forward | CCTCTGTTGCTATTCTCTGACATT |
| | Reverse | CTCGTAGTTGATAAAGTCGTCCTC |
| MRPL49 | Forward | TTGTGGAATCTGTGGATGAATACC |
| | Reverse | TGTACACCTCTACCTTGCGAAT |
| GAPDH | Forward | AGAAGGCTGGGGCTCATTTG |
| | Reverse | AGGGGCCATCCACAGTCTTC |

Statistics analysis

The 'ggpubr' package in R (version 0.6.0) was used for statistical analyses. To compare the mean differences in the PCR results and biochemical indicators, we used the unpaired Student's t test for normally distributed data and the Mann-Whitney U test for data that were not normally distributed. Additionally, we utilized the Spearman correlation coefficient to explore the associations between the expression of hub genes and the estimated glomerular filtration rate (eGFR), identifying potential associations with renal function. The threshold for statistical significance was set at a p value less than 0.05, ensuring that the observed differences and correlations were robust.

Results

DEG analysis

The initial differential analysis was conducted on the DKD datasets GSE30122. This analysis identified 3,086 DEGs with a threshold of $p < 0.05$. The full results of the DEG analysis are shown in Table S2. Using thresholds of an absolute \log_2 -FC greater than 1 and an adjusted p value less than 0.05, we selected 118 DEGs. Among these genes, 13 genes were downregulated and 105 were upregulated in DKD samples. The five upregulated genes with the greatest \log_2 -FC values were LTF, CXCL6, IGJ, C3 and MMP7, and the five downregulated genes with the greatest \log_2 -FC values were MAGI2, SST, 6PC, APOH and ETNPPL. The DEGs are visualized as volcano plots and heatmaps in Figure 1.

Identification of key gene modules via WGCNA

To construct a robust weighted co-expression network, we first determined the optimal soft thresholding parameter, β , to ensure a scale-free network. We established a β value of 7, which facilitated the construction of gene modules by

emphasizing strong correlations and penalizing weaker correlations (Figure 2a). Network construction was performed via dynamic tree cutting, merging gene modules with a similarity greater than 75% (distance < 0.25), resulting in a total of nine distinct gene modules (Figure 2b). Table S3 lists the module colors for each gene. The intermodule relationships are shown in Figure 2c. Correlation analysis between these modules and DKD traits was visualized with a heatmap (Figure 2d), illustrating the relationships among the modules. Notably, the brown module emerged as the most significant, exhibiting a correlation of 0.69 with DKD, a highly significant association (p value = $6.2E-11$). The brown module contained 495 genes, indicating a robust cluster of potentially critical drivers of DKD pathology.

Functional enrichment analysis of the brown module genes

To decipher the biological functions associated with the 495 genes in the brown module, we undertook comprehensive GO and KEGG pathway analyses. The full GO and KEGG analysis results can be found in Table S4. BP analysis revealed significant enrichment of pathways pivotal to immune functionality, including immune response-regulating signaling, leukocyte-mediated immunity, and positive regulation of cytokine production and cell activation Figure 3a. CC analysis indicated that these genes predominantly localize to the external side of the plasma membrane, collagen-containing extracellular matrix, and various granular membranes Figure 3b. MF enrichment analysis highlighted their roles as structural constituents of the extracellular matrix, immune receptors, and carbohydrate-binding agents Figure 3c. KEGG pathway analysis validated the immune-centric role of these genes, revealing significant enrichment in pathways such as cytokine-cytokine receptor interaction, phagosome formation, and leukocyte transendothelial migration, underscoring the involvement of these genes in key immunological processes Figure 3d.

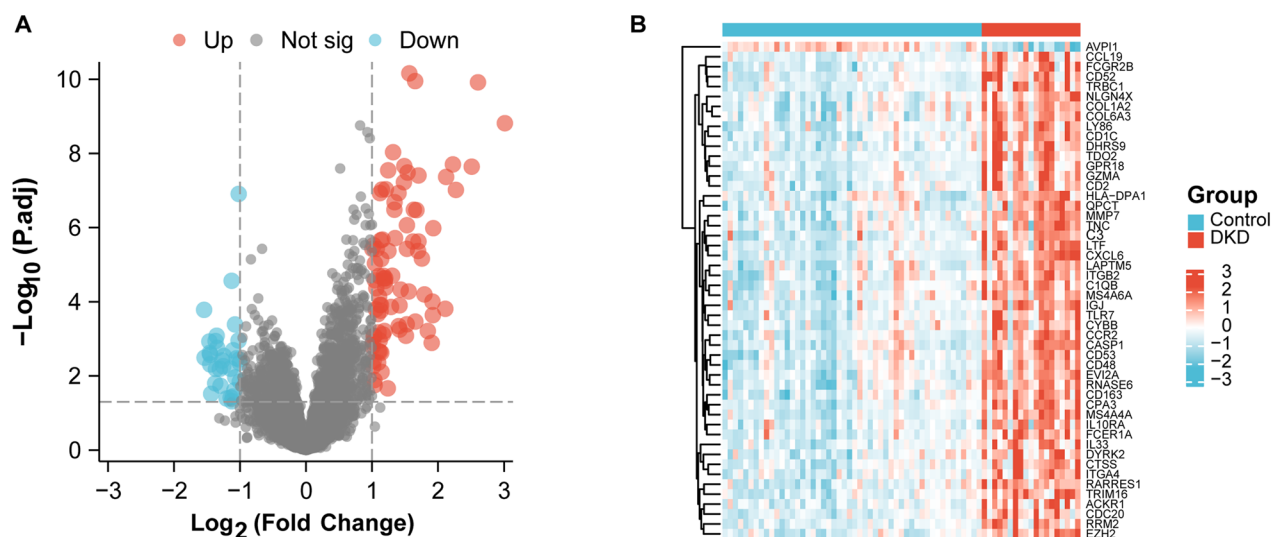


Figure 1. Differentially expressed genes in DKD.

a: Volcano plot illustrating the differentially expressed genes (DEGs) in GSE30122. b: Heatmap showing the expression patterns of the top 50 DEGs in GSE30122. The red dots represent upregulated genes, and the green dots represent downregulated genes.

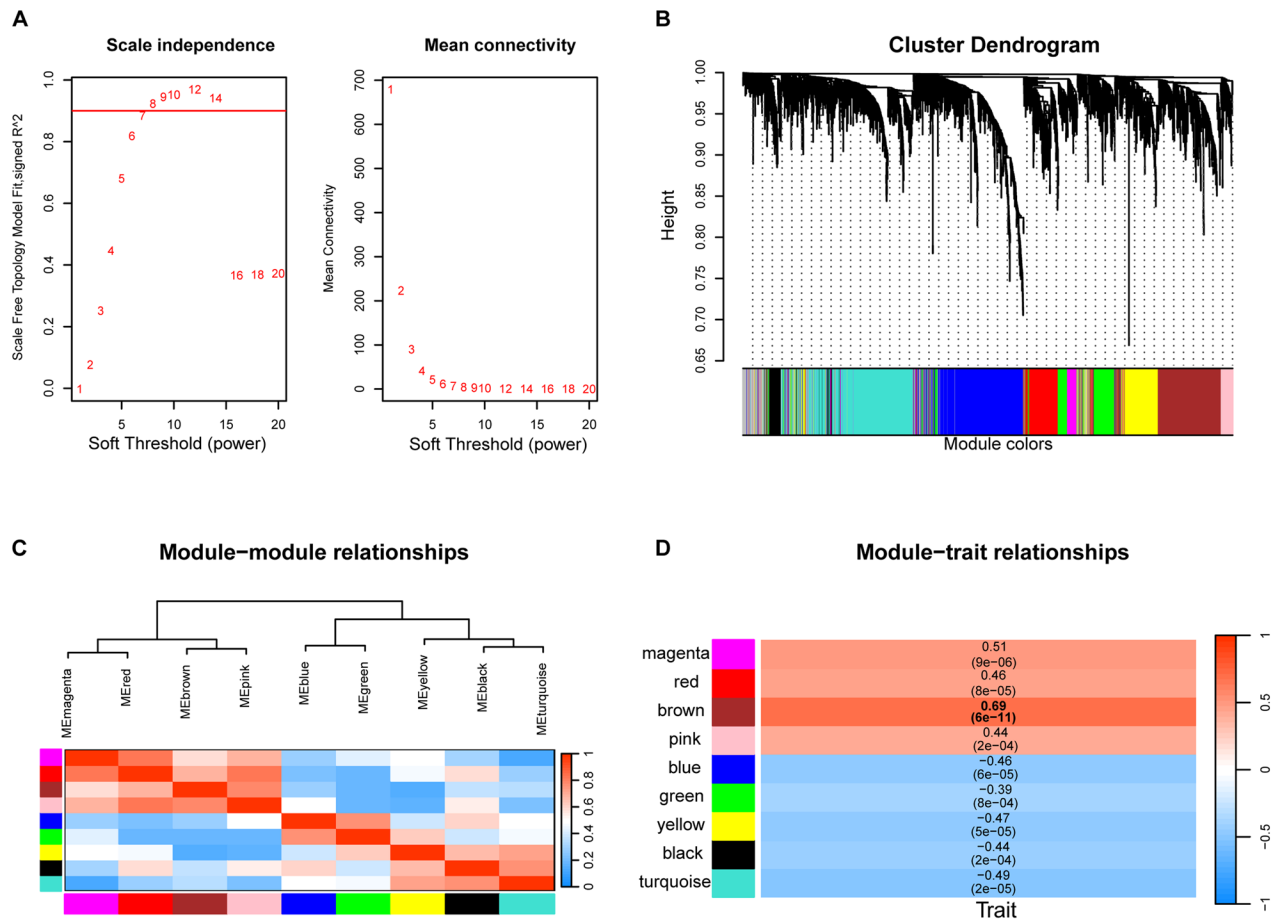


Figure 2. Weighted gene co-expression network analysis and module-trait relationships.

a: Determination of the soft-thresholding power β value, used for network construction to ensure a scale-free topology. b: Dendrogram illustrating gene clustering and module identification, with merging of closely related modules at a height cutoff of 0.25. c: Heatmap displaying the correlations among the nine identified gene modules. d: Correlation heatmap between DKD traits and each of the gene modules.

Key mitochondrial genes and immune infiltration

We obtained a list of mitochondrial-related genes from the MitoCarta3.0 database and identified genes that overlapped with those in the brown WGCNA module through Venn diagram analysis. This approach yielded 6 key mitochondrial genes implicated in DKD: MRPL49, CASP3, BCL2A1, EFHD1, AASS, and MPC1 (Figure 4a). Given the enrichment of the brown module genes in immune regulatory functions, we further explored immune cell dynamics in DKD. Immune cell infiltration analysis was performed to elucidate the immune landscape in DKD patients versus normal controls. The analysis revealed distinctive patterns of immune cell distribution; DKD patients presented increased levels of resting memory CD4+ T cells, M1 macrophages, and resting mast cells and decreased levels of memory B cells, monocytes, and activated mast cells (Figure 4b and c). Correlation studies between the identified key genes and various immune cells revealed several significant interactions. Notably, the expression level of BCL2A1 was positively correlated with the number of gamma delta T cells and activated dendritic cells. Conversely, the expression level of MRPL49 was negatively correlated with the number of naive B cells, and the expression level of CASP3 exhibited mixed interactions, being negatively correlated with the number of memory B cells but positively correlated with the number of

resting mast cells and gamma delta T cells. The expression levels of EFHD1 and AASS also demonstrated associations with multiple immune cell types. Interestingly, no significant correlations were detected between MPC1 and any immune cell type (Figure 4d).

Machine learning analysis of key mitochondrial genes in DKD

We employed machine learning algorithms to analyze the feature importance and predictive capabilities of the six key mitochondrial genes identified in the previous analyses. RF, SVM, and XGBoost methods were utilized to evaluate the importance of these genes and model their diagnostic potential for DKD. The results of each machine learning algorithm for the importance of the genes are presented in Table S5. RF analysis highlighted CASP3 and EFHD1 as the most influential genes, as assessed via the mean decrease Gini index (Figure 5a). ROC curve analysis demonstrated excellent predictive performance on the training set (AUC = 1.00) and robust performance on the test set (AUC = 0.87), confirming the model's effectiveness (Figure 5b). The SVM feature importance scores identified EFHD1 as the most

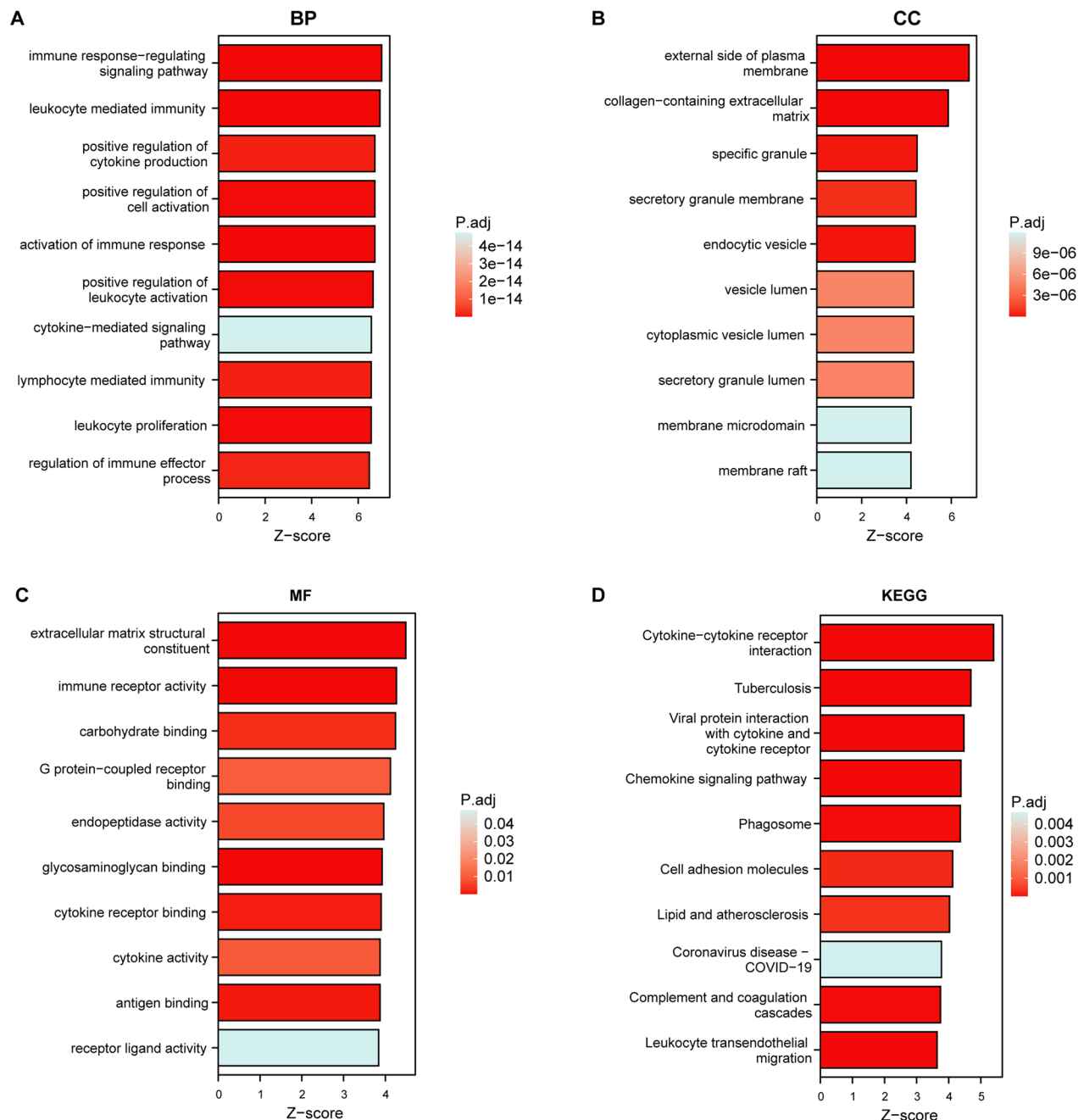


Figure 3. Functional enrichment of genes in the brown module.

a-c: Gene Ontology (GO) analysis depicting gene involvement across various biological process, cellular component, and molecular function terms. d: Kyoto Encyclopedia of Genes and Genomes (KEGG) pathway analysis, illustrating the primary pathways enriched among the module genes. The x-axis represents the z score, indicating the relative change in gene expression within each GO term, and the y-axis lists the enriched pathway terms.

positive contributor to the model, whereas CASP3 had a significant negative impact (Figure 5c). The SVM ROC curves reflected high accuracy in the training set (AUC = 0.984) and moderate accuracy in the test set (AUC = 0.710), suggesting specific conditions under which the SVM performance was optimized (Figure 5d). XGBoost analysis identified EFHD1 as having the greatest importance, followed by CASP3 and MRPL49 (Figure 5e). The ROC curves were outstanding in the training set (AUC = 1.00) and highly effective in the test set (AUC = 0.898), highlighting the robustness of XGBoost in handling complex datasets (Figure 5f).

Expression trends and clinical correlations of key genes

We investigated the expression patterns of key mitochondrial genes across different datasets to confirm their relevance in DKD. Figure 6a illustrates the variations in gene expression between healthy and DKD samples in the validation dataset GSE96804; as expected, all key genes demonstrated significant expression differences. Notably, genes such as AASS, EFHD1, MPC1, and MRPL49 consistently exhibited decreased expression in the DKD group in both the GSE30122 and GSE96804 datasets, whereas CASP3 expression was increased in DKD samples. Interestingly, the expression of BCL2A1 varied

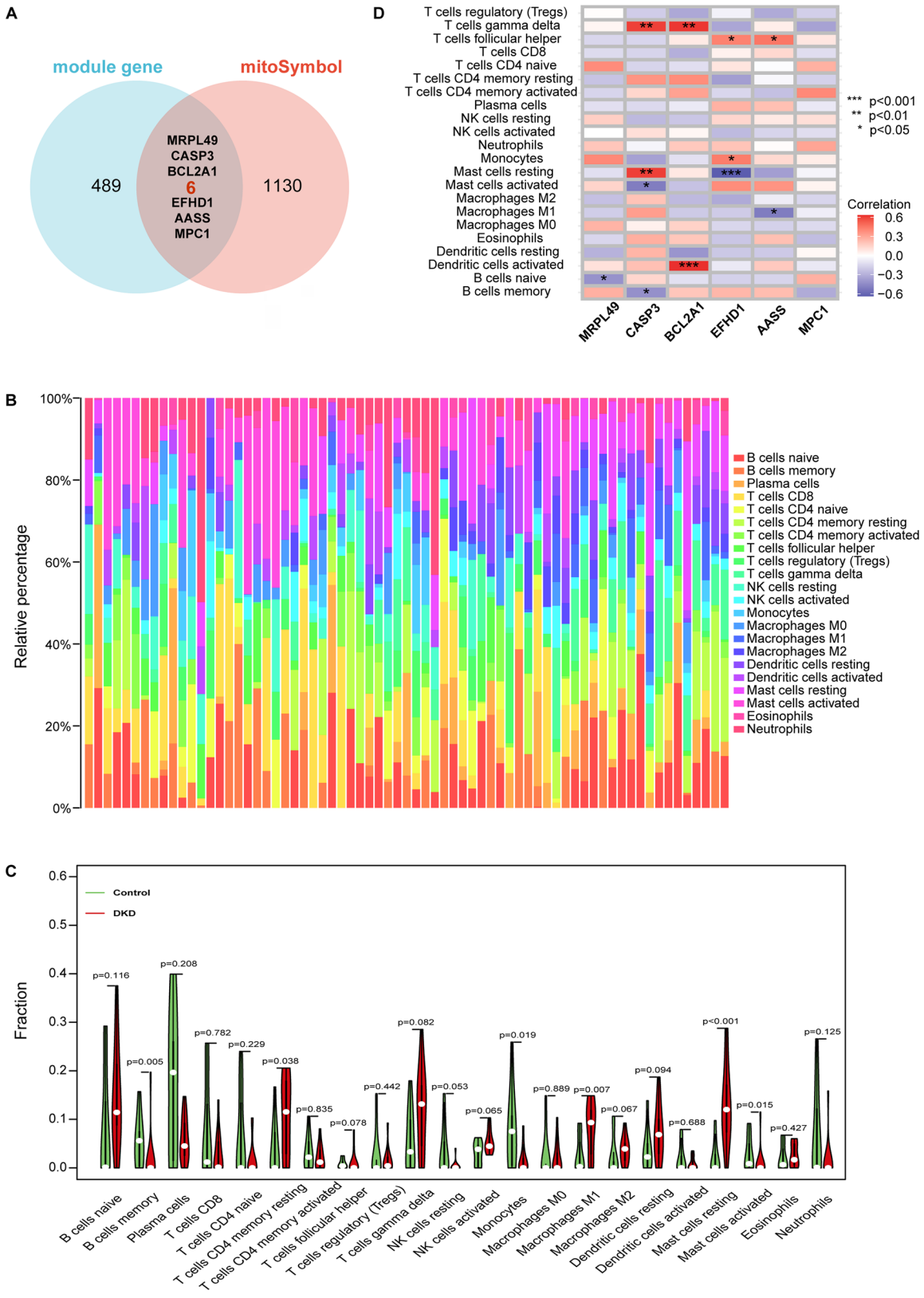


Figure 4. Mitochondrial-related genes and immune cell infiltration in DKD. a: Venn diagram showing key mitochondrial genes from the brown module. b: Distribution of 22 types of immune cells in DKD patients versus normal controls. c: Violin plots showing differential immune cell levels in DKD patients. d: Correlation heatmap of key mitochondrial genes with immune cell profiles.

between the datasets; the expression was higher in DKD samples in GSE30122 but lower in those in GSE96804. Further analysis *via* the Nephroseq online database was performed to

explore the relationships between these key genes and renal damage markers (Figure 6b). Correlation curves drawn from the DKD dataset indicated a negative correlation between the

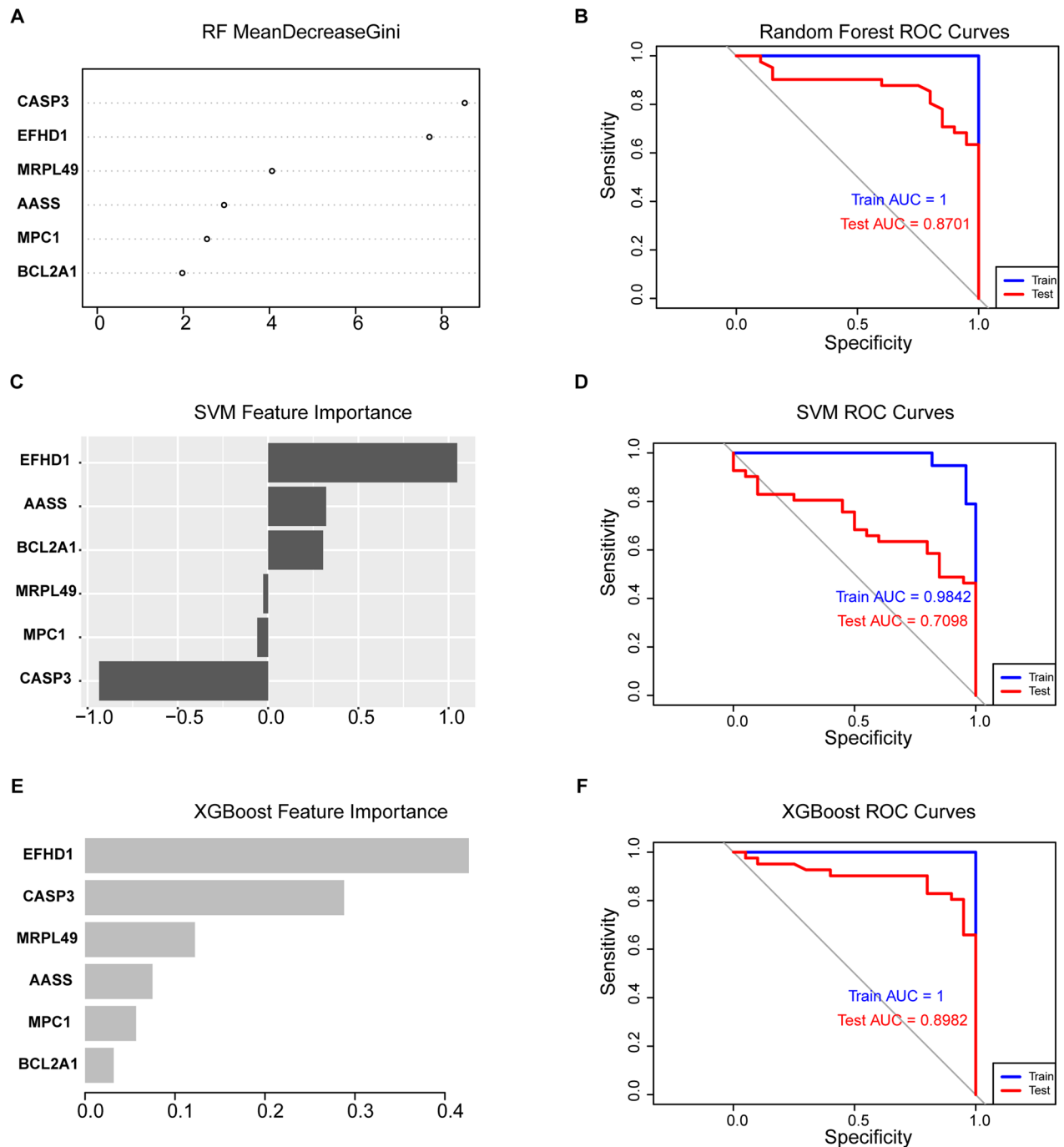


Figure 5. Machine learning analysis of key gene importance and predictive accuracy.

a, c, e: Feature importance plots for RF, SVM, and XGBoost, respectively. b, d, f: ROC curves for each model, illustrating their diagnostic accuracy across the training (GSE30122) and testing (GSE96804) datasets.

expression levels of AASS, EFHD1, MPC1, and MRPL49 and the serum creatinine level. Conversely, increased expression levels of CASP3 and BCL2A1 were closely associated with increased creatinine levels, suggesting their potential roles in the progression of renal impairment in DKD patients.

ROS levels and gene expression analysis in animal models

To validate our findings in an animal model of DKD, we initially measured the levels of ROS in both the control and

experimental groups. As shown in [Figure 7a](#), the ROS levels were significantly elevated in the experimental group compared with those in the control group ($p=0.0046$), confirming the occurrence of mitochondrial damage associated with DKD. We then used PCR to quantify the expression levels of five key genes in the two groups. The results revealed a marked increase in CASP3 expression in the DKD group compared with the control group ($p=0.0003$) ([Figure 7b](#)), which is consistent with previous studies that report the role of CASP3 in apoptosis and kidney damage in DKD. Notably,

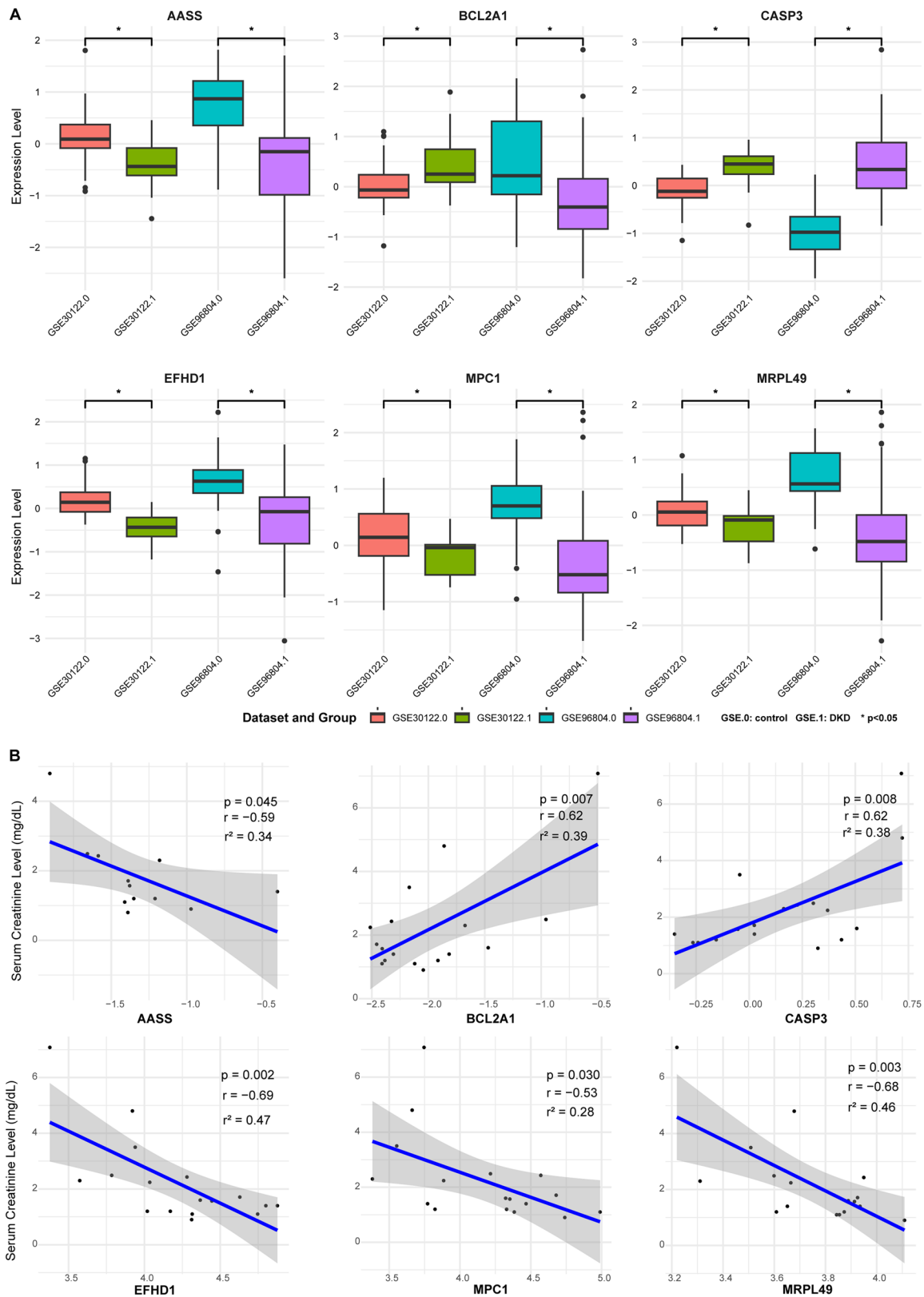


Figure 6. Expression and clinical correlation analysis of key genes associated with DKD.

a: Box plots showing the expression levels of key genes across datasets.

b: Correlation analysis between key gene (median-centered log₂) expression levels and serum creatinine levels via Nephroseq.

AASS expression was significantly reduced in the DKD group ($p=0.039$) (Figure 7c), which is consistent with our bioinformatics analysis and the online database results. Conversely,

the PCR results for the other three genes, EFHD1, MPC1, and MRPL49, did not support the earlier bioinformatics conclusions (Figure 7d-f). The observed differences may be due to

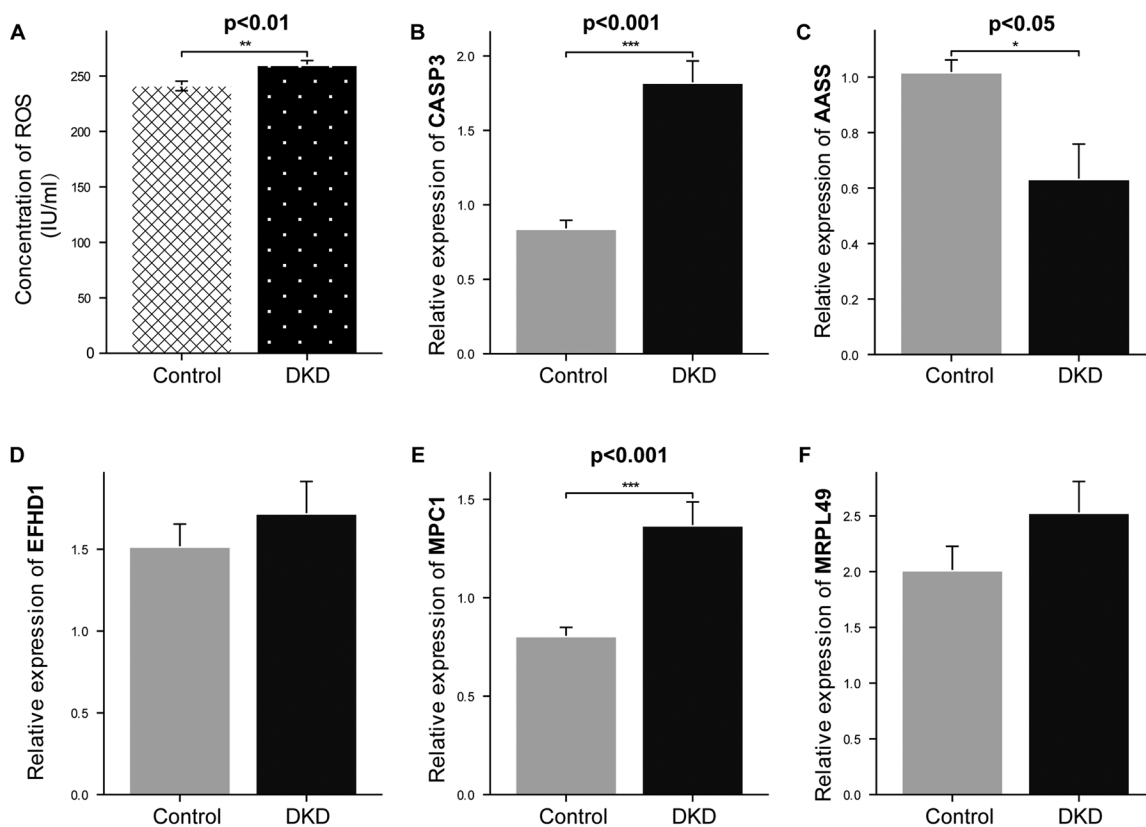


Figure 7. ROS levels and key gene expression analysis in DKD animal models.

a: Bar graph showing the ROS levels in the control and experimental groups.

b-f: Bar graphs depicting the PCR expression levels of five key genes in the control and DKD groups. DKD: diabetic kidney disease. $*p < 0.05$, $**p < 0.01$, $***p < 0.001$.

species variations between the human data and our animal models, as well as differences in experimental conditions. These discrepancies indicate that the involvement of these genes in DKD may be more intricate than initially understood and suggest the need for further investigation.

Discussion

DKD is a major debilitating complication of diabetes that often progresses to end-stage renal disease (ESRD) if untreated or poorly managed. DKD is characterized by a complex interplay of molecular and genetic alterations, including inflammation, oxidative stress, mitochondrial dysfunction, and apoptosis. These interwoven mechanisms contribute to the deterioration of kidney function and are critical for understanding the pathophysiology of the disease. Despite significant advances in our knowledge, the precise molecular pathways driving DKD remain incompletely understood, underscoring the need for continued research to identify novel biomarkers and therapeutic targets that can halt or even reverse disease progression.

In this study, we employed a multifaceted approach to elucidate the underlying genetic and molecular mechanisms of DKD. Through the analysis of publicly available datasets from the GEO, we identified a set of significant DEGs in DKD samples. Using WGCNA, we identified gene modules that were strongly associated with DKD traits, which provided a

deeper understanding of the molecular networks underlying the disease. The functional enrichment analysis of these DEGs highlighted immune response pathways and mitochondria-related genes, suggesting that mitochondrial dysfunction is a key driver of DKD progression. Immune cell infiltration analysis revealed distinct immune signatures in DKD patients compared with healthy controls, reinforcing the concept that immune dysregulation plays a significant role in the pathogenesis of DKD. Furthermore, machine learning algorithms were employed to predict key regulatory genes, increasing our ability to identify potential biomarkers and therapeutic targets. These findings were validated in animal models, in which increased levels of ROS and altered gene expression of candidate genes were observed. Our study integrates advanced bioinformatics tools, machine learning techniques, and experimental validation to provide a comprehensive molecular landscape of DKD, identifying critical genes and pathways that could inform future therapeutic strategies. The identification of key genes such as AASS and CASP3, their functional implications, and their potential as therapeutic targets provides valuable insights into the pathogenesis of DKD.

The CASP3 gene encodes a cysteine–aspartic acid protease that plays a crucial role in the execution of apoptosis [20]. CASP3 is a key effector in the apoptosis cascade that mediates the cleavage of various cellular substrates, ultimately leading to the characteristic morphological and

biochemical features of apoptosis. CASP3 is closely associated with mitochondrial function, particularly through its regulation of the permeability of the mitochondrial outer membrane. This process results in the release of cytochrome c into the cytosol, a key step in apoptosis. Cytochrome c binds to Apaf-1 to form the apoptosome, which subsequently activates caspase-9 and CASP3 and initiates the apoptotic pathway [21]. Additionally, mitochondrial proteins such as Smac/DIABLO and OMI/HtrA2 are released during apoptosis, further enhancing CASP3 activity by inhibiting inhibitors of apoptosis proteins (IAPs) [22]. CASP3 also directly affects mitochondrial function by cleaving mitochondrial inner membrane complexes, such as Complex I and Complex II. This cleavage leads to the loss of mitochondrial membrane potential and a decrease in ATP production, exacerbating apoptosis [23]. In the context of DKD, high glucose levels stimulate CASP3 cleavage and DNA fragmentation, leading to mesangial cell apoptosis and contributing to the progression of kidney damage [24]. Studies have shown that CASP3 expression and activity are significantly increased in DKD patients and correlated apoptosis, inflammation, and fibrosis [25]. The upregulation of CASP3 at the activity, protein, and mRNA levels suggests that apoptosis in DKD is likely CASP3 dependent. Therapeutic strategies targeting CASP3 have shown promise in ameliorating renal damage in DKD patients. For example, inhibition of CASP3 *via* Z-DEVD-FMK in STZ-induced diabetic mice reduced albuminuria, improved renal function, and attenuated tubulointerstitial fibrosis. These nephroprotective effects were associated with the inhibition of gasdermin E (GSDME)-dependent secondary necrosis, revealing a novel pathway through which CASP3 contributes to DKD progression [26]. Furthermore, pharmacological agents such as saxagliptin reduce renal apoptosis and pathological outcomes in DN by downregulating the expression of CASP3 and poly (ADP-ribose) polymerase-1 (PARP-1) in the death receptor pathway of apoptosis [27]. Similarly, LCZ696 (valsartan/sacubitril) has been reported to alleviate DKD by inhibiting inflammation and apoptosis, including reducing CASP3 activity and expression [28].

Several therapeutic strategies targeting CASP3 for the treatment of DKD have been developed. For example, the effectiveness of calcium dobesilate (CaD) in DKD patients is attributed to its potential mechanisms involving CASP3 regulation. CaD has shown the potential to alleviate kidney damage by affecting the CASP3-mediated apoptotic pathway [29]. Traditional Chinese medicine and other pharmacological agents have also been recognized for their ability to regulate CASP3 expression and activity, thereby improving renal outcomes [30–32]. CASP3 plays a critical role in apoptotic pathways leading to kidney cell loss and damage in DKD patients. Its involvement in the regulation of mitochondrial dynamics and inflammatory responses makes it a key target for therapeutic interventions.

The AASS gene encodes a bifunctional protein that catalyzes the first two steps of lysine degradation, converting lysine to alpha-amino adipic semialdehyde. This gene is crucial in the lysine degradation pathway, maintaining lysine

homeostasis and preventing the accumulation of lysine-related metabolites [33]. In DKD, the role of AASS in lysine degradation is particularly significant. Reduced expression of AASS in DKD patients can disrupt lysine metabolism, leading to the accumulation of toxic lysine catabolites, which may contribute to renal damage and disease progression. Since lysine metabolism is linked to the production of intermediates involved in cellular signaling and metabolic regulation, any imbalance could adversely affect various cellular functions essential for kidney health. Experimental evidence from murine hepatic cell lines shows that RNA interference (RNAi) targeting AASS decreases lysine catabolism, demonstrating the potential to manipulate AASS expression to modulate amino acid metabolism [34]. This approach could be explored as a therapeutic strategy in DKD patients to restore normal lysine levels and prevent the harmful effects of lysine accumulation. Furthermore, AASS is regulated through complex interactions between glucocorticoid receptors (GRs) and KLF15 in feed-forward loops (FFLs) [35]. These regulatory loops influence the expression of amino acid-metabolizing enzymes under hormonal control. The interplay between GRs and KLF15 and their binding affinities within glucocorticoid response elements (GREs) modulates AASS expression in response to hormonal signals. Hormonal imbalances and stress responses are common in DKD patients, and dysregulation of these loops could further impact AASS activity and lysine metabolism, contributing to disease progression. In addition to its role in lysine degradation, AASS has been implicated in various pathological conditions. In patients with steroid-sensitive nephrotic syndrome (SSNS), AASS expression is upregulated following glucocorticoid treatment, suggesting that AASS plays a role in mediating the body's response to these steroids [36]. This result contrasts with its expression in steroid-resistant nephrotic syndrome (SRNS), indicating that AASS expression may be critical in determining treatment outcomes. In DKD patients, inflammation and immune responses are significant, and understanding how AASS modulates glucocorticoid responses could provide insights that can help improve treatment strategies. AASS has also been identified as a key gene with significant predictive potential for insulin resistance. Its expression in skeletal muscle and intermuscular adipose tissue (IMAT) is strongly associated with clinical measures of glucose metabolism [37]. Given that insulin resistance is a common feature in DKD, the role of AASS in glucose metabolism highlights its potential as a biomarker for early detection and intervention in diabetic complications, including DKD [38]. The histone demethylase Ndy1/KDM2B promotes AASS expression, protecting cells from oxidative stress-induced apoptosis [39]. The role of AASS in redox regulation and cellular defence mechanisms indicates its importance in maintaining cellular health. In DKD, oxidative stress is a significant contributor to kidney damage, and increasing AASS expression could provide a protective effect against oxidative injury.

The role of AASS in disease mechanisms is closely linked to its relationship with mitochondria. AASS is associated with changes in mitochondrial morphology and energy metabolism

in embryonic stem cells (ESCs) [40]. Knockout studies of mitochondrial fission genes revealed that AASS, in addition to other genes, regulates ATP generation and maintains mitochondrial function. Studies in *Caenorhabditis elegans* and mice have shown that mutations in the saccharopine dehydrogenase (SDH) domain of AASS lead to mitochondrial damage due to increased saccharopine levels. This damage affects mitochondrial dynamics and overall development, highlighting the importance of saccharopine degradation in maintaining mitochondrial function [41–43]. In neurodegenerative disorders such as pantothenate kinase associated neurodegeneration (PKAN), mutations affecting mitochondrial phosphopantetheinyl-proteins, including AASS, lead to reduced expression levels and mitochondrial dysfunction [44]. Treatment with pantothenate can restore these protein levels, highlighting the role of AASS in mitochondrial health. In DKD patients, similar mechanisms of mitochondrial dysfunction may be at play, and restoring AASS function could mitigate mitochondrial damage and improve cellular health. The diverse roles of AASS in various human health conditions provide a comprehensive understanding of its metabolic, regulatory, and therapeutic implications. The involvement of AASS in DNA damage repair, mitochondrial function, redox regulation, and metabolic pathways underscores its potential as a biomarker and therapeutic target in DKD. Further research into the genetic variants and regulatory mechanisms of AASS will improve our understanding of its role in DKD and contribute to the development of targeted interventions to mitigate kidney damage and improve patient outcomes.

While our study provides valuable insights into the molecular mechanisms underlying DKD, several limitations should be acknowledged. First, our analysis relied primarily on bioinformatics approaches using existing datasets and validations in animal models. Although these methods are robust, they may not fully capture the complexity and heterogeneity of human DKD. The progression of DKD varies widely among individuals due to factors such as genetic predispositions, environmental influences, lifestyles, and comorbidities. Future studies should include larger cohorts of human patients to increase the statistical power and generalizability of the findings. Increasing the sample size would allow for a more comprehensive exploration of gene expression variability and could identify additional key genes involved in DKD pathogenesis. Second, our experimental validations were conducted using a single animal model, which may not have fully replicated the human disease condition. Comparative studies across multiple species could provide deeper insights into the conserved and divergent molecular mechanisms of DKD. The use of different animal models would help validate the relevance of the identified genes and pathways in various biological contexts, increasing the translational potential of our findings. Third, our study utilized bulk RNA sequencing data, which reflect average gene expression across heterogeneous cell populations. This approach may mask cell type-specific expression patterns and obscure the contributions of rare or specialized cell types. Single-cell RNA sequencing (scRNA-seq) offers the potential to resolve this

issue by providing high-resolution gene expression profiles at the individual-cell level. Future research employing scRNA-seq could elucidate the specific roles of mitochondrial dysfunction and immune dysregulation in different kidney cell types, such as podocytes, mesangial cells, and tubular epithelial cells. These findings could enhance our understanding of the cellular heterogeneity of DKD and identify cell type-specific therapeutic targets. Finally, while our findings highlight the importance of mitochondrial dysfunction and immune dysregulation in DKD, the precise molecular mechanisms linking these pathways to kidney damage remain to be fully elucidated. Detailed mechanistic studies, including functional assays and pathway analyses, are necessary to delineate how mitochondrial and immune pathways interact and contribute to DKD progression. In summary, addressing these limitations through larger, multispecies studies and advanced techniques such as single-cell sequencing will be crucial for validating our findings and translating them into effective clinical interventions for DKD.

Conclusion

This study provides a detailed molecular portrait of DKD, integrating differential gene expression, network analysis, immune profiling, machine learning, and animal model validation. The identification of key genes such as AASS and CASP3, their involvement in mitochondrial and immune pathways, and their clinical correlations offer valuable insights into the pathogenesis of DKD. These findings lay a robust foundation for future research aimed at developing targeted therapies to mitigate kidney damage and improve outcomes for patients with DKD.

Acknowledgements

The authors would like to thank the staff at the Affiliated Hospital of Qingdao University Biological Laboratory for their assistance in separating and submitting test samples. During the preparation of this work, the authors used ChatGPT to assist in drafting and refining the manuscript content. After using this tool, the authors reviewed and edited the content as needed and take full responsibility for the content of the publication.

Disclosure statement

No potential conflict of interest was reported by the author(s).

Ethics statement

In this study, we utilized publicly accessible GEO datasets. Ethical clearance for the original data collection was obtained from each contributing study's institutional review board, and all participants provided informed consent. This study was registered and approved by the ethics review board of the ethics committee of the Affiliated Hospital of Qingdao University (Ethics approval number: QYFY-WZLL-28888).

Funding

This research was supported by grants from the National Natural Science Foundation of China [82370724], the Qingdao Key Health Discipline Development Fund and the Qingdao Key Clinical Specialty Elite Discipline project.

Data availability statement

The datasets supporting the conclusions of this study are publicly available in the Gene Expression Omnibus (GEO) database. The microarray datasets GSE30122 and GSE96804 can be accessed at <https://www.ncbi.nlm.nih.gov/geo/>. Mitochondrial-related genes were sourced from the MitoCarta3.0 database, which is available at <https://www.broadinstitute.org/mitocarta/mitocarta30-inventory-mammalian-mitochondrial-proteins-and-pathways>. Additionally, clinical correlations of key genes were analyzed using the Nephroseq V5 platform, accessible at <https://www.nephroseq.org/resource/main.html>. Further details and additional data supporting the findings of this study are available from the corresponding author upon reasonable request.

References

- [1] Saelee R, Hora IA, Pavkov ME, et al. Diabetes prevalence and incidence inequality trends among U.S. adults, 2008–2021. *Am J Prev Med.* 2023;65(6):973–982. doi: [10.1016/j.amepre.2023.07.009](https://doi.org/10.1016/j.amepre.2023.07.009).
- [2] Di Marco M, Scilletta S, Miano N, et al. Cardiovascular risk and renal injury profile in subjects with type 2 diabetes and non-albuminuric diabetic kidney disease. *Cardiovasc Diabetol.* 2023;22(1):344. doi: [10.1186/s12933-023-02065-2](https://doi.org/10.1186/s12933-023-02065-2).
- [3] Gupta S, Dominguez M, Golestaneh L. Diabetic kidney disease: an update. *Med Clin North Am.* 2023;107(4):689–705. doi: [10.1016/j.mcna.2023.03.004](https://doi.org/10.1016/j.mcna.2023.03.004).
- [4] Yao L, Liang X, Qiao Y, et al. Mitochondrial dysfunction in diabetic tubulopathy. *Metabolism.* 2022;131:155195. doi: [10.1016/j.metabol.2022.155195](https://doi.org/10.1016/j.metabol.2022.155195).
- [5] Ahmad AA, Draves SO, Rosca M. Mitochondria in diabetic kidney disease. *Cells.* 2021;10(11):2945. doi: [10.3390/cells10112945](https://doi.org/10.3390/cells10112945).
- [6] Liu S, Yuan Y, Xue Y, et al. Podocyte injury in diabetic kidney disease: a focus on mitochondrial dysfunction. *Front Cell Dev Biol.* 2022;10:832887. doi: [10.3389/fcell.2022.832887](https://doi.org/10.3389/fcell.2022.832887).
- [7] Petrica L, Vlad A, Gadalean F, et al. Mitochondrial DNA changes in blood and urine display a specific signature in relation to inflammation in normoalbuminuric diabetic kidney disease in type 2 diabetes mellitus patients. *Int J Mol Sci.* 2023;24(12):9803. doi: [10.3390/ijms24129803](https://doi.org/10.3390/ijms24129803).
- [8] Mitrofanova A, Fontanella AM, Burke GW, et al. Mitochondrial contribution to inflammation in diabetic kidney disease. *Cells.* 2022;11(22):3635. doi: [10.3390/cells11223635](https://doi.org/10.3390/cells11223635).
- [9] Mohandes S, Doke T, Hu H, et al. Molecular pathways that drive diabetic kidney disease. *J Clin Invest.* 2023;133(4):e165654. doi: [10.1172/JCI165654](https://doi.org/10.1172/JCI165654).
- [10] Zhang X, Zhang J, Ren Y, et al. Unveiling the pathogenesis and therapeutic approaches for diabetic nephropathy: insights from panvascular diseases. *Front Endocrinol.* 2024;15:1368481. doi: [10.3389/fendo.2024.1368481](https://doi.org/10.3389/fendo.2024.1368481).
- [11] Chen J, Liu Q, He J, et al. Immune responses in diabetic nephropathy: pathogenic mechanisms and therapeutic target. *Front Immunol.* 2022;13:958790. doi: [10.3389/fimmu.2022.958790](https://doi.org/10.3389/fimmu.2022.958790).
- [12] Li Y-X, Lu Y-P, Tang D, et al. Anthocyanin improves kidney function in diabetic kidney disease by regulating amino acid metabolism. *J Transl Med.* 2022;20(1):510. doi: [10.1186/s12967-022-03717-9](https://doi.org/10.1186/s12967-022-03717-9).
- [13] Zhang X, Chao P, Zhang L, et al. Single-cell RNA and transcriptome sequencing profiles identify immune-associated key genes in the development of diabetic kidney disease. *Front Immunol.* 2023;14:1030198. doi: [10.3389/fimmu.2023.1030198](https://doi.org/10.3389/fimmu.2023.1030198).
- [14] Luo Y, Zhang L, Zhao T. Identification and analysis of cellular senescence-associated signatures in diabetic kidney disease by integrated bioinformatics analysis and machine learning. *Front Endocrinol (Lausanne).* 2023;14:1193228. doi: [10.3389/fendo.2023.1193228](https://doi.org/10.3389/fendo.2023.1193228).
- [15] Woroniecka KI, Park ASD, Mohtat D, et al. Transcriptome analysis of human diabetic kidney disease. *Diabetes.* 2011;60(9):2354–2369. doi: [10.2337/db10-1181](https://doi.org/10.2337/db10-1181).
- [16] Pan Y, Jiang S, Hou Q, et al. Dissection of glomerular transcriptional profile in patients with diabetic nephropathy: SRGAP2a protects podocyte structure and function. *Diabetes.* 2018;67(4):717–730. doi: [10.2337/db17-0755](https://doi.org/10.2337/db17-0755).
- [17] Langfelder P, Horvath S. WGCNA: an R package for weighted correlation network analysis. *BMC Bioinformatics.* 2008;9(1):559. doi: [10.1186/1471-2105-9-559](https://doi.org/10.1186/1471-2105-9-559).
- [18] Rath S, Sharma R, Gupta R, et al. MitoCarta3.0: an updated mitochondrial proteome now with sub-organelle localization and pathway annotations. *Nucleic Acids Res.* 2021;49(D1):D1541–D1547. doi: [10.1093/nar/gkaa1011](https://doi.org/10.1093/nar/gkaa1011).
- [19] Chen B, Khodadoust MS, Liu CL, et al. Profiling Tumor Infiltrating Immune Cells with CIBERSORT. *Methods Mol Biol.* 2018;1711:243–259. doi: [10.1007/978-1-4939-7493-1_12](https://doi.org/10.1007/978-1-4939-7493-1_12).
- [20] Nicholson DW, Ali A, Thornberry NA, et al. Identification and inhibition of the ICE/CED-3 protease necessary for mammalian apoptosis. *Nature.* 1995;376(6535):37–43. doi: [10.1038/376037a0](https://doi.org/10.1038/376037a0).
- [21] Walsh JG, Cullen SP, Sheridan C, et al. Executioner caspase-3 and caspase-7 are functionally distinct proteases. *Proc Natl Acad Sci USA.* 2008;105(35):12815–12819. doi: [10.1073/pnas.0707715105](https://doi.org/10.1073/pnas.0707715105).
- [22] Das S, Shukla N, Singh SS, et al. Mechanism of interaction between autophagy and apoptosis in cancer. *Apoptosis.* 2021;26(9–10):512–533. doi: [10.1007/s10495-021-01687-9](https://doi.org/10.1007/s10495-021-01687-9).
- [23] Mitra S, Anand U, Jha NK, et al. Anticancer applications and pharmacological properties of piperidine and piperine: a comprehensive review on molecular mechanisms and therapeutic perspectives. *Front Pharmacol.* 2022;12:772418. doi: [10.3389/fphar.2021.772418](https://doi.org/10.3389/fphar.2021.772418).
- [24] Mishra R, Emancipator SN, Kern T, et al. High glucose evokes an intrinsic proapoptotic signaling pathway in mesangial cells. *Kidney Int.* 2005;67(1):82–93. doi: [10.1111/j.1523-1755.2005.00058.x](https://doi.org/10.1111/j.1523-1755.2005.00058.x).
- [25] Yang B, El Nahas AM, Thomas GL, et al. Caspase-3 and apoptosis in experimental chronic renal scarring. *Kidney Int.* 2001;60(5):1765–1776. doi: [10.1046/j.1523-1755.2001.00013.x](https://doi.org/10.1046/j.1523-1755.2001.00013.x).
- [26] Wen S, Wang ZH, Zhang CX, et al. Caspase-3 promotes diabetic kidney disease through gasdermin E-mediated progression to secondary necrosis during apoptosis.

- Diabetes Metab Syndr Obes. 2020;13:313–323. doi: [10.2147/DMSO.S242136](https://doi.org/10.2147/DMSO.S242136).
- [27] Xing X, Guo S, Liu Y, et al. Saxagliptin protects against diabetic nephropathy by inhibiting caspase 3/PARP-1-dependent nephrocyte apoptosis. *Exp Ther Med*. 2021;22(3):990. doi: [10.3892/etm.2021.10422](https://doi.org/10.3892/etm.2021.10422).
- [28] Mohany M, Ahmed MM, Al-Rejaie SS. The role of NF- κ B and Bax/Bcl-2/Caspase-3 signaling pathways in the protective effects of sacubitril/Valsartan (Entresto) against HFD/STZ-induced diabetic kidney disease. *Biomedicines*. 2022;10(11):2863. doi: [10.3390/biomedicines10112863](https://doi.org/10.3390/biomedicines10112863).
- [29] Du B, Yin Y, Wang Y, et al. Calcium dobesilate efficiency in the treatment of diabetic kidney disease through suppressing MAPK and chemokine signaling pathways based on clinical evaluation and network pharmacology. *Front Pharmacol*. 2022;13:850167. doi: [10.3389/fphar.2022.850167](https://doi.org/10.3389/fphar.2022.850167).
- [30] Wang J, Ma G, Zhang P, et al. Mechanism of Huaiqihuang in treatment of diabetic kidney disease based on network pharmacology, molecular docking and in vitro experiment. *Medicine (Baltimore)*. 2023;102(50):E36177. doi: [10.1097/MD.00000000000036177](https://doi.org/10.1097/MD.00000000000036177).
- [31] Zhang SJ, Zhang YF, Bai XH, et al. Integrated network pharmacology analysis and experimental validation to elucidate the mechanism of acteoside in treating diabetic kidney disease. *Drug Des Devel Ther*. 2024;18:1439–1457. doi: [10.2147/DDDT.S445254](https://doi.org/10.2147/DDDT.S445254).
- [32] Gao Y, Guo Z, Liu Y. Analysis of the potential molecular biology of triptolide in the treatment of diabetic nephropathy: a narrative review. *Medicine*. 2022;101(48):E31941. doi: [10.1097/MD.00000000000031941](https://doi.org/10.1097/MD.00000000000031941).
- [33] Sacksteder KA, Biery BJ, Morrell JC, et al. Identification of the alpha-aminoaliphatic semialdehyde synthase gene, which is defective in familial hyperlysinemia. *Am J Hum Genet*. 2000;66(6):1736–1743. doi: [10.1086/302919](https://doi.org/10.1086/302919).
- [34] Cleveland BM, Kiess AS, Blemings KP. Alpha-aminoaliphatic delta-semialdehyde synthase mRNA knockdown reduces the lysine requirement of a mouse hepatic cell line. *J Nutr*. 2008;138(11):2143–2147. doi: [10.1093/jn/138.11.2143](https://doi.org/10.1093/jn/138.11.2143).
- [35] Sasse SK, Zuo Z, Kadiyala V, et al. Response element composition governs correlations between binding site affinity and transcription in glucocorticoid receptor feed-forward loops. *J Biol Chem*. 2015;290(32):19756–19769. doi: [10.1074/jbc.M115.668558](https://doi.org/10.1074/jbc.M115.668558).
- [36] Bhayana S, Zhao Y, Merchant M, et al. Multiomics analysis of plasma proteomics and metabolomics of steroid resistance in childhood nephrotic syndrome using a ‘patient-specific’ approach. *Kidney Int Rep*. 2023;8(6):1239–1254. doi: [10.1016/j.ekir.2023.03.015](https://doi.org/10.1016/j.ekir.2023.03.015).
- [37] Lutter D, Sachs S, Walter M, et al. Skeletal muscle and intermuscular adipose tissue gene expression profiling identifies new biomarkers with prognostic significance for insulin resistance progression and intervention response. *Diabetologia*. 2023;66(5):873–883. doi: [10.1007/s00125-023-05874-y](https://doi.org/10.1007/s00125-023-05874-y).
- [38] Penno G, Solini A, Orsi E, et al. Insulin resistance, diabetic kidney disease, and all-cause mortality in individuals with type 2 diabetes: a prospective cohort study. *BMC Med*. 2021;19(1):66. doi: [10.1186/s12916-021-01936-3](https://doi.org/10.1186/s12916-021-01936-3).
- [39] Polyarchou C, Pfau R, Hatzia Apostolou M, et al. The JmjC domain histone demethylase Ndy1 regulates redox homeostasis and protects cells from oxidative stress. *Mol Cell Biol*. 2008;28(24):7451–7464. doi: [10.1128/MCB.00688-08](https://doi.org/10.1128/MCB.00688-08).
- [40] Seo BJ, Choi J, La H, et al. Role of mitochondrial fission-related genes in mitochondrial morphology and energy metabolism in mouse embryonic stem cells. *Redox Biol*. 2020;36:101599. doi: [10.1016/j.redox.2020.101599](https://doi.org/10.1016/j.redox.2020.101599).
- [41] Gatrell SK, Berg LE, Barnard JT, et al. Tissue distribution of indices of lysine catabolism in growing swine. *J Anim Sci*. 2013;91(1):238–247. doi: [10.2527/jas.2011-5070](https://doi.org/10.2527/jas.2011-5070).
- [42] Guo Y, Wu J, Wang M, et al. The metabolite saccharopine impairs neuronal development by inhibiting the neurotrophic function of glucose-6-phosphate isomerase. *J Neurosci*. 2022;42(13):2631–2646. doi: [10.1523/JNEUROSCI.1459-21.2022](https://doi.org/10.1523/JNEUROSCI.1459-21.2022).
- [43] Zhou J, Wang X, Wang M, et al. The lysine catabolite saccharopine impairs development by disrupting mitochondrial homeostasis. *J Cell Biol*. 2019;218(2):580–597. doi: [10.1083/jcb.201807204](https://doi.org/10.1083/jcb.201807204).
- [44] Álvarez-Córdoba M, Talaverón-Rey M, Villalón-García I, et al. Down regulation of the expression of mitochondrial phosphopantetheinyl-proteins in pantothenate kinase-associated neurodegeneration: pathophysiological consequences and therapeutic perspectives. *Orphanet J Rare Dis*. 2021;16(1):201. doi: [10.1186/s13023-021-01823-3](https://doi.org/10.1186/s13023-021-01823-3).